Silencing c-*MYC* Expression by Targeting Quadruplex in P1 Promoter Using Locked Nucleic Acid Trap[†]

Niti Kumar,[‡] Ashok Patowary,[‡] Sridhar Sivasubbu,[‡] Michael Petersen,[§] and Souvik Maiti*[,‡]

Institute of Genomics and Integrative Biology, CSIR, Mall Road, Delhi 110007, India, and Nucleic Acid Center, Department of Physics and Chemistry, University of Southern Denmark, 5230 Odense M, Denmark

Received June 5, 2008; Revised Manuscript Received October 10, 2008

ABSTRACT: The nuclease hypersensitive element of P1 promoter in *c-MYC* gene harbors a potential of unusual structure called quadruplex, which is involved in molecular recognition and function. This Hoogsteen bonded structure is in dynamic equilibrium with the usual Watson−Crick duplex structure, and these competing secondary structures undergo interconversion for execution of their respective biological roles. Herein, we investigate the sensitivity of the *c-MYC* quadruplex−duplex equilibrium by employing a locked nucleic acid (LNA) modified complementary strand as a pharmacological agent. Our biophysical experiments indicate that the c-*MYC* quadruplex under physiological conditions is stable and dominates the quadruplex−WC duplex equilibrium in both sodium and potassium buffers. This equilibrium is perturbed upon introducing the LNA modified complementary strand, which demonstrates efficient invasion of stable *c-MYC* quadruplex and duplex formation in contrast to the unmodified complementary strand. Our data indicate that LNA modifications confer increased thermodynamic stability to the duplex and thus favor the predominance of the duplex population over that of the quadruplex. Further, we demonstrate that this perturbation of equilibrium by a pharmacological agent results in altered gene expression. Our in vivo experiment performed using the LNA modified complementary strand suggests the influence of the quadruplex−duplex structural switch in the modulation of gene expression. We believe that this exploratory approach utilizing the selectivity and specificity of Watson−Crick base pairing of LNA bases would allow the modulation of quadruplex regulated gene expression.

The *c-MYC* gene has stimulated interest and research activities because of its potential role as a protoncogene (*1, 2*). This gene codes for MYC oncoprotein, which affects cellular growth, differentiation, and apoptosis (*3, 4*). The MYC protein undergoes post-translational modifications such as phoshorylation, acetylation, and ubiquitinylation (*5*). These modifications affect its stability, modulate its molecular functions as a transcriptional regulator, and define its interactions with other proteins involved in transcription machinery and signaling pathways. The cellular choice between growth and differentiation requires a fine balance between *c-MYC* stimulation and repression. Deregulation in *c-MYC* expression leads to genetic instability and oncogenesis (*5, 6*). The transcription of *c- MYC* is initiated from two major start sites, P1 and P2, which are separated by 161 bp in the human *c-MYC* gene (*7*). The nuclease hypersensitivity element (NHE) III of the P1 promoter controls c-*MYC* transcription and has been the subject of intense research over the past few decades (*7*). The NHE III of the *c-MYC* region contains guanine stretches, which assemble to form quadruplexes containing the planar array of Hoogsteen bonded guanine quartets (*8, 9*). However, the presence of the complementary strand suggests the potential existence of a usual secondary structure, Watson−Crick duplex. This implies that both the quadruplex and duplex exist in equilibrium and undergo interconversion to execute their respective biological roles. The facile transformation of the guanine-rich sequence of the NHE III in the *c-MYC* promoter from the Watson−Crick duplex to a kinetically favored G-quadruplex may act as a transcriptional switch in gene expression. Thus, targeting or perturbing this quadruplex−Watson−Crick duplex equilibrium can modulate *c-MYC* expression. Guanine-rich sequences are also found in other DNA regions such as telomeres, centromeres, immunoglobulin switch regions, mutational hot spots, and other promoter elements in the human genome and have the potential to form four-stranded structures (*10*−*13*). These unusual structures involved in molecular recognition and function have an intricate role to play both at the DNA and RNA levels in regulating gene expression (*10*−*16*). The possible existence and roles of G-quadruplexes in vivo have been corroborated by the detection of several proteins such as helicases and nucleases that bind specifically to G-quadruplexes (*17, 18*). The increasing evidence of quadruplexes being implicated in disease has kindled interest in developing synthetic ligands that can bind selectively to these structures, affect their molecular recognition properties and allow their application as a therapeutic target (*19, 20*). However, these quadruplex-interacting ligands do not display high selectivity toward the

[†] N.K., A.P., S.S., and S.M. acknowledge CSIR (Structure−function relation of modified nucleic acids and Facility Creation Project- FAC 02) for funding this research. M.P. acknowledges The Danish National Research Foundation for financial support.

* To whom correspondence should be addressed. Phone: +91-11-2766-6156. Fax: +91-11-2766-7471.. E-mail: souvik@igib.res.in.

[‡] Institute for Genomics and Integrative Biology.

[§] University of Southern Denmark.

10.1021/bi801064j CCC: $40.75
Published on Web 11/17/2008

Scheme 1: Role of Quadruplex−WC Duplex Equilibrium in the P1 Promoter on c-*MYC* Expression

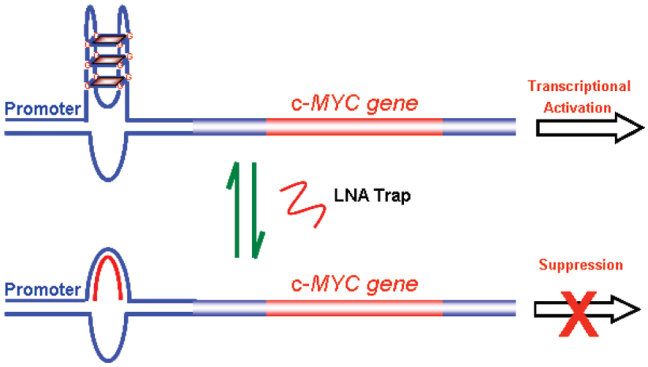

quadruplex over duplex and are unable to discriminate between quadruplexes adopted by different sequences. Another attractive strategy to affect their molecular recognition and function may involve engineering the unfolding of these stable structures by employing a nucleic acid based approach, which would allow discriminative unfolding of different quadruplexes. Efforts are being invested in developing synthetic nucleic acids that can hybridize to G-rich sequence through Watson−Crick base pairing and thus act as therapeutic agents. Recently, invasion of the DNA and RNA quadruplex was demonstrated through complementary and homologous peptide nucleic acid (PNA) probes (*21*−*23*). Among the nucleic acid analogues, locked nucleic acid (LNA), a conformationally locked analogue, displays unprecedented high affinity toward its target and also provides increased thermostability to duplexes and triplexes (*24*−*29*). LNA outscores other nucleic acid analogues because of its ability to exhibit biological stability without being associated with toxic effects and thus may facilitate artificial control of gene expression in vivo (*30*). Herein, we demonstrate that perturbation of the quadruplex−duplex equilibrium by a pharmacological agent results in altered gene expression (Scheme 1). To establish this, we have employed a LNA modified complementary strand, and through biophysical methods, we demonstrate efficient invasion of a stable *c-MYC* quadruplex and duplex formation by a modified complementary strand in contrast to its DNA counterpart. Further, we performed in vivo experiments to affirm the influence of the quadruplex−duplex structural switch in the modulation of gene expression.

MATERIALS AND METHODS

Oligonucleotides. Dual labeled and single labeled G-rich oligonucleotides were obtained from Microsynth. Unmodified and LNA modified complementary strands were obtained from Exiqon. All of the oligonucleotides were HPLC purified. The concentrations of unlabeled oligonucleotides were calculated by extrapolation of tabulated values of the monomer bases and dimers at 25 °C using procedures reported earlier (*31, 32*).

NMR Spectroscopy. The NMR experiment was recorded on a Varian Inova 500 spectrometer. The 22-mer c-*MYC* quadruplex was prepared by heating it for 5 min at 90 °C followed by slow annealing to room temperature in 90% H_2O/10% D_2O solution (pH 7.4) and 100 mM NaCl. The quadruplex concentration was 0.2 mM. One dimensional (1D) Watergate NOESY spectra were recorded at 25 °C. The spectrum was acquired with ca. 29,000 scans.

CD Spectra. The CD spectrum of the c-*MYC* 22-mer quadruplex (5 μM) was recorded using a Jasco 715 spectropolarimeter at 25 °C. The sample was prepared by slow annealing in 10 mM sodium cacodylate buffer at pH 7.4 and 100 mM NaCl.

UV Melting Study. The c-*MYC* quadruplex sample was prepared by heating the oligonucleotides in 10 mM sodium cacodylate buffer at pH 7.4, 100 mM NaCl, and 140 mM KCl followed by slow cooling. Melting experiment was performed with 3 μM concentration in a Cary 400 (Varian) spectrophotometer equipped with a Hitachi SPR-10 thermoprogrammer with a heating rate of 0.2 °C/min. Data was collected at 295 nm.

Fluorescence Study. Fluorescence experiments were performed at 25 °C in a Fluoromax 4 (spex) spectrofluorimeter for dual labeled 5′ fluorescein GGGGAGGGTGGGGA GGGTGGGG TAMRA 3′. In the Fluoromax 4 (spex) spectrofluorimeter, excitation wavelength was set at 480 nm, and emission was recorded from 500−700 nm. Samples were prepared in 10 mM sodium cacodylate buffer at pH 7.4 and 100 mM NaCl. Through steady state kinetics experiments at 25 °C, we observed that kinetics of duplex formation in sodium and potassium buffer attains a presaturation phase within 1 and 3 h, respectively. Spectra were recorded for samples containing preformed quadruplex (100 nM) and equimolar concentration of unmodified and LNA modified complementary strands after 1 h of incubation in 100 mM NaCl buffer at 25 °C. Similarly, samples were prepared in 140 mM KCl, and an experiment was performed in 10 mM sodium cacodylate buffer and 140 mM KCl with 3 h of incubation at 25 °C.

A FLUOstar OPTIMA fluorescence plate reader was used to determine the binding affinity of the G-quadruplex to its complementary strand as described previously (*43*). The experiments were done in 384 well plates, using excitation (480 nm) and emission (520 nm) filters for fluorescein. The wells were loaded with the solution of fixed concentration of preformed quadruplex (100 nM) and with increasing concentrations of the complementary strand (0 to 1.5 μM). For analysis of data, the observed fluorescence intensity was considered as the sum of the weighted contributions from the folded G-quadruplex strand and extended G-strand in duplex form:

$$F = (1 - \alpha b)F_0 + \alpha_b F_b \qquad (1)$$

where F is the observed fluorescence intensity at each titrant concentration, F_0 and F_b are the respective fluorescence intensities of initial and final states of titration, and α_b is the mole fraction of quadruplex in duplex form. Assuming 1:1 stoichiometry for the interaction in the case of complementary strand binding, it can be shown that

$$[Q]_0\alpha_b^2 - ([Q]_0 + [C] + 1/K_A)\alpha_b + [C] = 0 \qquad (2)$$

where K_A is the association constant, $[Q]_0$ is the total G-strand concentration, and [C] is the added complementary strand concentration.

From eqs 1 and 2, it can be shown that

$$\Delta F = \left(\frac{\Delta F_{max}}{2[Q]_0}\right)\left\{\left([Q]_0 + [C] + \frac{1}{K_A}\right) - \sqrt{\left([Q]_0 + [C] + \frac{1}{K_A}\right)^2 - 4[Q]_0\,[C]}\right\} \quad (3)$$

where $\Delta F = F - F_0$ and $\Delta F_{max} = F_{max} - F_0$.

Nondenaturing Gel Electrophoresis. The quadruplex was prepared using 5′ fluorescein GGGGAGGGTGGGGAGGGTGGGG 3′ by heating at 95 °C, followed by slow annealing in 100 mM NaCl and 140 mM KCl buffer. Preformed quadruplex (1.5 μM) was incubated with equimolar concentrations of unmodified and LNA modified complementary strands in 10 mM sodium cacodylate buffer at pH 7.4 and 100 mM NaCl for 3 h at 4 °C. The samples were electrophoresed on 15% polyacrylamide nondenaturing gel and run in 1× TBE at pH 7.4 and 100 mM NaCl buffer. The gel was run at 4 °C at a constant voltage of 100 V. Similarly, gel electrophoresis was performed in 140 mM KCl buffer with equimolar and 10 times excess of complementary strand concentration with 5 h of incubation at 4 °C. The gel was visualized in a Fujifilm phosphorimager using a 480 nm laser and a 520 nm filter, and relative intensities of the bands were determined.

Surface Plasmon Resonance Study. SPR measurements were performed with a BIAcore 2000 (BIAcore Inc.) system using streptavidin-coated sensor chips (Sensor chip SA; BIAcore Inc.). The 31mer 5′-biotin TTTTTTTTTGGGGAGGGTGGGGAGGGTGGGG-3′ was heated to 95 °C and annealed by slow cooling to form the quadruplex in filtered and degassed 10 mM HEPES with 100 mM NaCl with 0.005% surfactant IGEPAL at pH 7.4. This sample was then immobilized (≈300 RU) on flow cell 2. Flow cell 1 was left blank as a control to account for any signal generated because of the bulk solvent effect or any other effect not specific to the DNA interaction, which was subtracted from the signal obtained in flow cell 2. All experiments were performed at 25 °C using running buffer (filtered and degassed 10 mM HEPES with 100 mM NaCl and 0.005% surfactant IGEPAL) at pH 7.4. Oligonucleotide immobilized surface was exposed to the running buffer for at least 2 h at a flow rate of 5 μL/min for attaining baseline stability. Analyte (unmodified and modified complementary strands) solutions at different concentrations (1.25 nM−200 nM) were prepared in the running buffer and were injected (at 20 μL/min for 300 s) in random series to avoid any systematic error, using an automated protocol. Following this, dissociation from the surface was monitored for 300 s in running buffer. Regeneration was done using 1 M NaCl in 50 mM NaOH. Data were analyzed using BIAevaluation 3.1.1.

Under pseudo-first-order conditions, where the free analyte concentration is held constant in the flow cell, the binding is described by

$$dR/dt = kaC(R_{max}\text{-}R)\text{-}k_dR \quad (4)$$

where dR/dt is the rate of change of the SPR response signal, R and R_{max} are the measured and maximum reponse signal measured with binding, C is the analyte concentration, and k_a and k_d are the association and dissociation rates, respectively. The binding constant, K_A is calculated as k_a/k_d. At equilibrium, $dR/dt = 0$, and eq 3 can be written as

$$R_{eq}/C = K_AR_{max}\text{-}K_AR_{eq} \quad (5)$$

$$R_{eq} = R_{max}K_AC/(1 + K_AC) \quad (6)$$

R_{eq} is the measured response at equilibrium, and values of R_{eq} are obtained at a series of injected analyte C concentrations. The steady state response when plotted versus analyte concentrations and fitted to the Langmuir isotherm for a molecular interaction provides the binding affinity of the immobilized molecule to its target and R_{max}.

Luciferase Assay. The Del 4 plasmid used in this study contains a 2.5 kb genomic fragment encompassing a minimal c-*MYC* promoter upstream of a luciferase cassette. Map of c-*MYC* promoter showing restriction sites used to generate deletion constructs is provided in Supporting Information, Figure 7. P1 and P2 are transcription start sites with P2 being the major start site. Del 4 plasmid containing the 22-mer Guanine rich target sequence upstream of luciferase reporter (*33*) was used in this study. This 22-mer quadruplex forming sequence was targeted using unmodified (DNA) and LNA modified (LNA 2 and LNA 5) complementary strand, and downstream reporter activity was assayed. We also performed experiments in which the flank sequences adjacent to the 22-mer quadruplex motif were also targeted with their respective complementary strands (Table 3). Luciferase reporter activity was assayed using zebrafish embryos. Zebrafish embryos were collected within 15 min of spawning and were placed on cooled agarose loading trays as described (*34, 35*). These plates are prechilled to 4 °C to slow initial embryonic cleavages. The agarose loading tray provides a soft and moist surface for the embryos. The microinjection apparatus used in the experiments is the same as that used by Hyatt et al. (*36*). The needles used in microinjection were made by pulling the glass capillaries in a Sutter P87 instrument. The needle was backloaded with 2−3 μL of injection solution by using elongated pipet tips (Eppendorf, Cat. No. 5242 956.003). While loading, air bubbles were avoided as it can affect the accuracy of injection. Prior to injection, the needle was calibrated using the Harward Apparatus (PLI 90) pico injector to regulate the drop size. The pico injector was set for the defined time pulse, and the needle tip was clipped with a jeweler's forcep (Sigma Aldrich Cat. No. F6521-1EA) to create an opening. Drop size was tested after each break until the desired calibration was achieved. After opening the end of the needle, drop solution was transferred to a microcapillary (Drummond, Cat. No. 1-000-0010) to quantify the drop volume. The microcapillary tube holds approximately 30 nL in 1 mm. The needle tip was clipped until the drop reaches a desired volume of 1 mm. The picoinjector controls were set for a 100 ms pulse to obtain the 3 nL dropsize. Calibrating the needle by this method provides consistency in the volume delivered to each embryo.

The Del 4 plasmid (25 pg/embryo) was coinjected with unmodified (2.5 pg/embryo) and LNA modified complementary strands (2.5 pg/embryo) in Zebrafish embryos using the method described previously (*35, 37*). This makes the target (plasmid)/oligo (complementary strand) molar concentration ratio as 1:50. The control experiment included embryos with (a) no plasmid and (b) Del 4 plasmid alone without any complementary strand, and (c) Del 4 plasmid and 22-mer nonspecific C-rich sequence d(CCCTTACCCTTACCCTTACCCT). After 24 h of incubation, the embryos

Table 1: Binding Parameters for the Hybridization of the c-*MYC* Quadruplex to Its Complementary Strand Determined through Fluorescence Study at 25 °C[a]

	sequence 5′-3′	no. of mod	F [b]	F [b]	K_A[c] (10^6M $^{-1}$)	D_{eq}[c] (%)
Q	GGGGAGGGTGGGGA GGGTGGGG		1.00	1.00		
DNA	CCCCACCCTCCCCACCCTCCCC	0	1.08	1.50	2.00 ± 0.18	14.60
LNA 1	**C**CCCACC**C**TCCCCAC**C**CTC**C**CC	4	1.14	2.25	6.80 ± 0.20	31.70
LNA 2	C**C**CCAC**C**CTCC**C**CAC**C**CTCC**C**C	5	1.20	2.50	10.00 ± 0.15	38.20
LNA 3	**C**CC**C**ACC**C**TCC**C**CAC**C**CTC**C**CC	6	1.22	2.25	13.00 ± 0.25	42.70
LNA 4	CCC**CA**CCCTCCC**CA**CCC**TC**CCC	6	1.33	2.75	32.00 ± 0.21	57.60
LNA 5	CCC**CA**CCC **TCCCCA**CCC**TC**CCC	10	1.37	3.50	55.00 ± 0.20	65.60

[a] LNA1−LNA5 are complementary strands with modifications represented as boldface underlined text. [b] The steady state fluorescence study was performed upon addition of equimolar concentrations of the complementary strand (100 nM) to the preformed quadruplex in 10 mM sodium cacodylate buffer, 140 mM KCl, and 100 mM NaCl at pH 7.4, respectively. F represents the ratio to acceptor intensity ($I_{520\ nm}/I_{585\ nm}$) for equimolar mixture of quadruplex and its complementary strand after normalization by fluorescence ratio ($I_{520\ nm}/I_{585\ nm}$) of the quadruplex alone. For complete duplex formation at 25 °C, the ratio I_{520nm}/I_{585nm} was observed to be 4.8. This was obtained for a mixture of preformed quadruplex and 15 times excess of the complementary strand to achieve complete duplex formation as observed from the binding data. [c] K_A is the equilibrium constant for duplex formation calculated in 100 mM NaCl. D_{eq} is the percentage of duplex formation determined at equilibrium when equimolar concentration of preformed quadruplex and complementary strand (100 nM) were mixed together in 10 mM sodium cacodylate buffer and 100 mM NaCl at pH 7.4. The amount of duplex at equilibrium, D_{eq}, was calculated from the binding affinity toward the complementary strand obtained at experimental conditions, using the equation $K_A = D_{eq}/(Q_0 - D_{eq}) \times (C_0 - D_{eq})$, where Q_0 and C_0 ($Q_0 = C_0$) are the initial quadruplex and complementary strand concentration.

were collected frozen at −80 °C for 1 h. The frozen embryos were crushed and homogenized in 1× CCLR buffer (Promega Luciferase Assay System Cat no: # E1500) with continuous pipetting at 4 °C for 30 min. The homogenate was centrifuged for 2 min at 10,000*g*. The supernatant is used for protein estimation by the bicinchoninic acid (BCA) method (*38*). Luciferase assay was performed in Orion Microplate Luminometer (Berthold Detection System) for three biological replicates using 50 μg of protein for all samples.

RESULTS AND DISCUSSION

The target sequence used in this study is a 22-mer purine rich sequence of NHE III of the c-*MYC* promoter located −143 to −110 bp upstream of the P1 promoter (Table 1). The 1D NMR spectrum (Supporting Information, Figure 1) of this sequence recorded in 100 mM NaCl shows a broad imino resonance at 10−12 ppm, indicating the presence of multiple interconverting conformers (chair and basket fold or propeller-type) (*8, 9*). The CD spectrum in 100 mM NaCl depicts the existence of a predominantly parallel and a small antiparallel population (Supporting Information, Figure 2) and is in agreement with previous reports (*9*). The UV melting profile shows that the element forms a stable quadruplex structure (Supporting Information, Figure 3A). To investigate the invasion of this quadruplex structure, we used a pyrimidine rich complementary strand modified with LNA bases. Systematic LNA modifications (Table 1) were incorporated in the complementary strand to drive quadruplex invasion and duplex formation. Modifications were incorporated in the pyrimidine strand at positions complementary to guanine bases in tetrads as well as to bases in the lateral and diagonal loops of the quadruplex structure. FRET (fluorescence resonance energy transfer) was employed using a dual labeled 22-mer purine rich sequence of NHE III of the c-*MYC* promoter. Upon addition of equimolar concentrations of the complementary strand to the preformed quadruplex, the fluorescence intensity at 520 nm corresponding to fluorescein increased, whereas that for TAMRA (at 585 nm) decreased in all cases as shown in Figure 1A. The ratio of donor to acceptor intensity ($I_{520\ nm}/I_{585\ nm}$) presented in Table 1 for the quadruplex in the presence of the complementary strand has been normalized by the fluorescence ratio (I_{520}

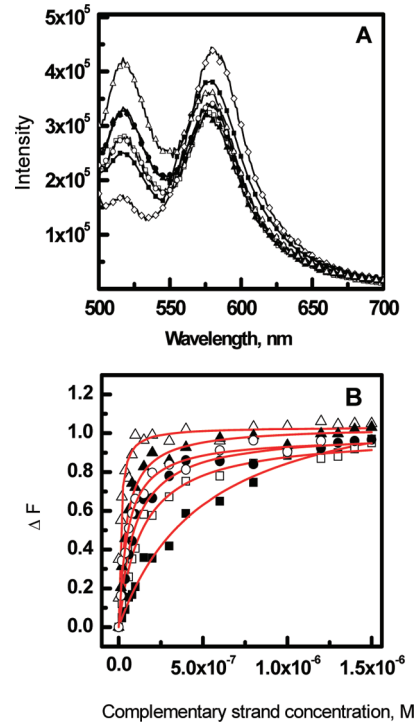

FIGURE 1: (A) Fluorescence spectra of dual labeled 22-mer c-*MYC* quadruplex (100 nM) with 5′ fluorescein and 3′ TAMRA in the absence (◇) and presence of equimolar concentrations of unmodified and modified complementary strand DNA (■), LNA 1 (□), LNA 2 (●) and LNA 3 (○), LNA 4 (▲), and LNA 5 (Δ) in 100 mM NaCl buffer at pH 7.4 and 25 °C. (B) Normalized fluorescence of the quadruplex (100 nM) at 520 nm as a function of complementary strand concentrations, DNA (■), LNA 1 (□), LNA 2 (●) and LNA 3 (○), LNA 4 (▲), and LNA 5 (Δ) in 10 mM sodium cacodylate buffer at pH 7.4 and 100 mM NaCl at 25 °C. The fluorescence change reflects the opening of the quadruplex for duplex formation.

$_{nm}/I_{585\ nm}$) of the quadruplex alone. Thus, the normalized fluorescence ratio ($I_{520\ nm}/I_{585\ nm}$) obtained from an equimolar mixture of preformed quadruplex and complementary strand reflects the relative duplex formation. The increase in this ratio upon addition of the LNA modified complementary strand suggested greater duplex formation for the LNA modified strand in contrast to the unmodified strand. For evaluating the efficiency of LNA modified complementary strands to invade and accelerate unfolding of the stable

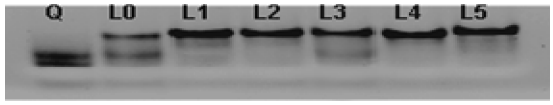

FIGURE 2: Gel electrophoresis for single labeled 22-mer c-*MYC* quadruplex with 5′ fluorescein (1.5 μM) in the absence and presence of equimolar concentrations of unmodified and modified complementary strands in 100 mM NaCl buffer at pH 7.4 and 4 °C. Q represents the quaduplex alone and L0 to L5 represents DNA to LNA 5.

c-*MYC* quadruplex to form the duplex, we assessed the binding affinity of the complementary strands to quadruplex. We monitored the change in fluorescence intensity of fluorescein with increasing complementary strand concentration (0 to 1.5 μM) in 100 mM NaCl buffer. Figure 1B represents the relative fluorescence intensity change (ΔF) as a function of the complementary strand concentration. The difference in the profile of relative fluorescence intensity change (ΔF) obtained for c-*MYC* quadruplex reflects the amount of duplex formed upon hybridization of the quadruplex to its complementary strand. The plot represented in Figure 1B was used to calculate the binding affinity of quadruplexes to their complementary strands using eq 3. The binding affinity of the preformed quadruplex toward the unmodified DNA and the modified LNA complementary strands are provided in Table 1. Using the association binding constants (K_A) obtained from the fluorescence study, we evaluated the amount of duplex formed in a mixture of equimolar concentration of preformed quadruplex and its complementary strand (Table 1). Best performance was observed for LNA 5 with 10 LNA modified nucleotides, which drive maximum duplex formation (Table 1). To obtain equivalent duplex formation as in the case of LNA 5, 15 times excess of the DNA unmodified strand was required in NaCl buffer (Figure 1B).

Next, we performed nondenaturing gel electrophoresis (Figure 2) to observe the conversion of the quadruplex to duplex. The presence of two discrete bands for quadruplex signifies the existence of mixed conformers in NaCl buffer, concordant with our NMR and CD observations. Addition of equimolar concentration of the complementary strand to the preformed quadruplex showed considerable residual quadruplex population (≈45%). This population decreased in the case of modified strands, with LNA 1 and LNA 3 showing ≈10% and ≈25% remaining quadruplex population, respectively. LNA 5 with maximum modifications showed almost entire conversion of quadruplex to duplex. These observations establish that the LNA modified complementary strand allows better conversion of quadruplex to duplex and that the amount of this conversion is dictated by the number and position of modification. Apart from the number of modified bases, the position of these modified bases is important to derive superior performance and requires further investigation.

Subsequently, we employed the surface plasmon resonance technique to obtain the kinetic parameters involved in quadruplex hybridization to its complementary strand to form duplex. The analysis of the sensorgram indicates an increase in association rate (k_a) and a simultaneous decrease in dissociation rate (k_d) upon increase in the number of LNA modifications (Table 2, Supporting Information, Figure 6). The association and dissociation rates for the quadruplex hybridization to unmodified DNA complementary strand were 1.5×10^5 M^{-1} s^{-1} and 1.0×10^{-3} s^{-1}, respectively. However, in the case of LNA 5 having maximum number of modifications, an increase in association rate to 4.6×10^5 M^{-1} s^{-1} and a concomitant decrease in dissociation rate to 0.31×10^{-3} s^{-1} were observed (Table 2). The plot of the measured response unit at equilibrium, R_{eq}, versus complementary strand concentrations, when fitted to Langmuir isotherm for molecular interactions, provides the binding affinity (Figure 3) and the maximum response at saturation of binding sites, which collectively reflect the amount of duplex formed. Greater binding affinity obtained for the modified complementary strand implies greater duplex forming capacity over that of the unmodified DNA strand. Though the increase in the number of LNA modifications increases the binding affinity of the complementary strand toward the quadruplex, the position of modifications also influences the efficiency of quadruplex invasion to form the duplex. LNA 5, with maximum LNA modifications has a binding affinity one order higher than that of DNA. Thus, the LNA modified strand has the ability to drive greater duplex formation in comparison to equivalent concentration of the unmodified DNA strand. The binding affinity for the hybridization of the preformed quadruplex to its unmodified and LNA modified complementary strands obtained from fluorescence was less than the values obtained from the SPR method (Tables 1 and 2). The difference in the binding affinities from fluorescence and SPR may arise because of the fact that in SPR experiments the quadruplex has been immobilized onto a sensor chip surface through a T_9 linker. Such immobilization often destabilizes DNA structures, and thus, it may have better binding toward its complementary strands showing higher binding affinities than those obtained by fluorescence methods. Other factors, such as probe density, surface heterogeneity, and nonspecific adsorption onto a sensor chip, may cause discrepancy in the binding affinity measurements.

Furthermore, we also performed biophysical experiments in potassium buffer. As the quadruplex formed in potassium buffer was highly stable (T_m = 75 °C; Supporting Information, Figure 3B), it was extremely difficult to unfold the quadruplex-K^+ in the presence of equimolar complementary strand concentration. We performed fluorescence and gel experiments at equimolar concentrations of quadruplex and complementary strands in 140 mM KCl buffer (Supporting Information, Figures 4 and 5). The fluorescence experiment performed in 140 mM KCl buffer showed only a slight increase in $I_{520\ nm}/I_{585\ nm}$ ratio (Supporting Information, Figure 4, Table 1). Our gel experiment shows that at equimolar concentrations of preformed quadruplex and its complementary strand in potassium buffer, the LNA modified strand showed better performance than the unmodified strand but could not drive complete duplex formation. We observed that at 10 times excess of the complementary strand, the LNA modified strand could achieve complete duplex formation in contrast to the unmodified strand. It has been reported previously by Fox and co-workers that 50-fold excess of DNA complementary strand is required to achieve complete conversion of c-*MYC* quadruplex to duplex in potassium buffers (*39*). It is noteworthy to mention that in vitro at equimolar concentration, LNA modified complementary strands are not effective in disrupting c-*MYC* quadruplex

Table 2: Kinetic Parameters for the Hybridization of the c-*MYC* Quadruplex to Its Complementary Strand Determined through SPR Study at 25 °C[a]

	sequence 5′-3′	no. of mod	k_a ($M^{-1}s^{-1}$) 10^5	k_d (s^{-1}) 10^{-3}	K_A (M^{-1}) 10^8
DNA	CCCCACCCTCCCCACCCTCCCC	0	1.50	1.00	1.5
LNA 1	**C**CCCACC**C**TCCCCAC**C**CTC**C**CC	4	4.50	0.86	5.2
LNA 2	C**C**CCAC**C**CTCC**C**CAC**C**CTCC**C**C	5	6.50	0.65	10.0
LNA 3	**C**CC**C**ACC**C**TCC**C**CAC**C**CTC**C**CC	6	3.80	0.77	5.0
LNA 4	CCC**CA**CCCTCCC**CA**CCC**TC**CCC	6	2.10	0.28	7.5
LNA 5	CCC**CA**CCC **TCCCCA**CCC**TC**CCC	10	4.60	0.31	15.0

[a] Sensorgrams were obtained in 10 mM HEPES buffer and 100 mM NaCl at pH 7.4. k_a and k_d are association and dissociation rate constants, respectively. K_A is the equilibrium association constant for duplex formation obtained by k_a/k_d. The values obtained by the SPR study are within 15% error.

Table 3: Sequences Used to Target the Flanking Regions of Quadruplex Motif for Reporter Assay[a]

	sequence 5′−3′ (22-mer)
flank 1a	CCCAAAGCAGAGGGCGTGGGGG
flank 1b	GCTAGAGTGCTCGGCTGCCCGG
flank 2a	ATAAGCGCCCCTCCCGGGTTCC
flank 2b	GGCTGAGTCTCCTCCCCACCTT
flank 3a	TCCCCATAAGCGCCCCTCCCGG
flank 3b	AGTCTCCTCCCCACCTTCCCCA

[a] Luciferase reporter activity was monitored upon targeting the flank regions of quadruplex motif at both 5′ and 3′ ends with their respective complementary strands. Flanks 1a and 1b are sequences complementary to a region 20 bases away from the quadruplex motif, flanks 2a and 2b are sequences complementary to the adjoining regions lying in the immediate vicinity of the motif, and flanks 3a and 3b are sequences complementary to the flank region including the 5 bases of the quadruplex motif.

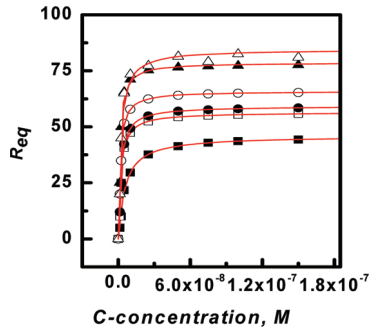

FIGURE 3: Plot of binding response R_{eq} versus complementary strand concentration DNA (■), LNA 1 (□), LNA 2 (●) and LNA 3 (○), LNA 4 (▲), and LNA 5 (Δ). The oligo was immobilized (≈300 RUs) on streptavidin-coated sensor chips. The experiments were performed in 10 mM HEPES and 100 mM NaCl at 25 °C.

structure, but they demonstrate an efficacious effect at lower concentrations in contrast to the unmodified complementary strand.

Except for the single stranded 3′ telomeric overhang, the G-rich strand is accompanied by its complementary C-rich strand, which thereby results in competitive equilibria between quadruplex and duplex structures. Quadruplex formation is favored over that of duplex formation especially under transient conditions such as replication, transcription, and recombination. Our biophysical experiments indicate that the c-*MYC* quadruplex under physiological conditions is stable and predominates in quadruplex−WC duplex equilibrium in both sodium and potassium buffers. In this context, the desired interrogation is whether the quadruplex−WC duplex structural switch has any role in the modulation of gene expression under physiological conditions. As a proof of the concept, we conducted in vivo experiments in zebrafish, where this equilibrium was perturbed using a pharmacological agent. Zebrafish has become a well-established vertebrate model organism for the identification and characterization of genes and pathways involved in human development, organ function, behavior, and diseases such as cancer (*40*−*42*). Other advantages of zebrafish includes transparent embryos and ex utero development of the embryo, which makes it easy to perform rapid screening of the pharmacological agent, conditional and tissue specific expression, and identification of transgenic zebrafish. The large number of studies on cancer development in zebrafish comes from transgenic zebrafish expressing mammalian oncogenes. This approach makes use of another advantage of zebrafish as a laboratory animal, the convenience of introducing foreign DNA into zebrafish cells and getting it expressed by injection into one-cell embryos. The plasmid containing the 22-mer target sequence upstream of the luciferase reporter gene (Supporting Information, Figure 7) was injected in zebrafish embryos in the absence and presence of unmodified (DNA) and LNA modified (LNA 2 and LNA 5) complementary strands and with a 22-mer nonspecific strand. The luciferase assay showed the suppression of luciferase expression for both unmodified and modified complementary strands in contrast to the plasmid alone. However, the modified strand caused greater magnitude of suppression of luciferase expression in comparison to unmodified complementary strand (Figure 4). The amount of suppression of the luciferase expression was proportional to the number of LNA modifications (DNA < LNA 2 < LNA 5). During transcription, the unwinding of two strands may allow the G-rich sequence upstream of luciferase reporter to adopt the intramolecular secondary structure. The presence of the complementary strand might interfere with quadruplex formation by driving the structural transition to duplex. This prevents quadruplex mediated regulation and results in the suppression of downstream gene expression. The LNA modified complementary strand could mediate greater suppression of gene expression (Scheme 1). The excellent performance of the LNA modified complementary strand in vivo can be credited to its higher biological stability and better hybridization ability, in comparison to that of the unmodified strand. These properties of LNA modified strands facilitate efficient invasion of stable quadruplex structure and better structural transition to duplex. To corroborate that the observed in vivo effect is mediated through quadruplex−duplex transition, we performed experiments where the flank regions of the quadruplex motif was targeted at both 5′ and 3′ ends with their respective unmodified complementary strands. The regions targeted included (i) flanking sequences 20 bases away from the quadruplex motif, (ii) adjoining regions lying in the immediate vicinity of the motif, and (iii)

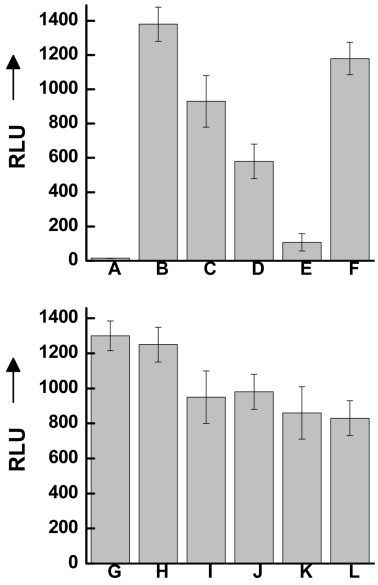

FIGURE 4: Luciferase assay performed with the Del 4 plasmid. (A) no plasmid, (B) Del 4 alone, (C) Del 4+DNA, (D) Del 4+LNA 2, (E) Del 4+LNA 5, (F) Del 4+nonspecific oligo, (G−H) flanks 1a and b, (I−J) flanks 2a and b, and (K−L) flanks 3a and b.

the region overlapping the flank sequences and quadruplex motif (Table 3). Our results show that targeting the flank region 20 bases away from the quadruplex motif site at both ends does not affect the downstream reporter activity (Figure 4G−H). However, targeting the flank region adjoining the quadruplex motif with the complementary strand affects the reporter activity moderately (Figure 4 I−J), and targeting the overlapping sequences results in significant decrease in reporter activity (Figure 4 K−L). The flank sequences have been associated with the overhang effect, which assists the invasion and disruption of stable quadruplex structure (*59*). Hence, targeting the flank bases proximal or overlapping with the quadruplex motif with their respective complementary strands destabilizes the motif and facilitates quadruplex−duplex transition, which perturbs gene expression. In our study, we did not observe a significant difference in reporter activity upon targeting either ends of the quadruplex motif; however, the importance of the 5′ and 3′ ends of the c-*MYC* quadruplex motif in quadruplex−duplex structural transition needs further investigation.

To address the influence of quadruplex−duplex equilibrium in the modulation of gene expression, we investigated the sequence from the nuclease hypersensitive region of the P1 promoter of the c-*MYC* gene. Several workers have demonstrated the potential of this region to form a quadruplex structure (*8, 9*). Our biophysical studies showed the superior ability of the LNA modified oligonucleotides to target the quadruplex, which resulted in the enrichment of duplex DNA in contrast to the unmodified counterpart (Table 1). We next tried to use the LNA modified oligonucleotides in vivo to interfere with the formation of the quadruplex. Quadraplex formation happens when the G-rich regions are transiently released from the constraint of duplex DNA during events such as transcription, thus acting as molecular recognition motifs. Therefore, selective targeting of the homopurine strand, which forms the quadruplex, using its complementary oligonucleotide results in the loss of Hoogsteen bonded quadruplex and the formation of the Watson−Crick duplex (*43−45*). This would perturb the molecular recognition by the transcription factor and hence might affect the downstream expression of the gene. Previous studies using in vitro polymerase assays and in vivo luciferase assays have demonstrated a transcription repressive role of the c-*MYC* quadruplex (*8*). The in vitro assay measures the potential of the secondary structure to block elongation by the polymerase and does not simulate eukaryotic transcription initiation. A second line of evidence from in vivo cell culture based luciferase assays shows that mutating the upstream region results in increased reporter gene expression in immortalized cell lines. In our system, during the normal development of zebrafish, disruption of the quadruplex decreased the expression of the downstream reporter gene. Therefore, the results from our preliminary in vivo experiments using the zebrafish system are apparently contradictory to the previous reports. The difference between our results and previous reports in the role of the c-*MYC* quadruplex can be explained in several ways. First, the c-*MYC* quadruplex has been established as a repressor element by using quadruplex stabilizing cationic porphyrin, which leads to transcriptional suppression of c-*MYC* (*8*). However, the possibility of the quadruplex stabilizing molecule perturbing the molecular recognition of the c-*MYC* quadruplex motif and competing with transcription factors leading to its transcriptional repression cannot be ruled out. Furthermore, the cationic porphyrin does not display high selectivity for the quadruplex over the duplex (*46*) and may also contribute toward nonquadruplex mediated effects. Second, the differences in trans-activating factors present in the cell lines and zebrafish system could account for the known repressive role and novel activating role reported here. The evidence taken together suggests that the quadruplex may act as a transcription-inducing or -repressing signal, depending on its context. It is noteworthy that transcription factors and regulatory elements are known to have dual roles of a repressor and activator (*47−50*). Recently, the dual role as transcriptional repressor and activator has been demonstrated for the GGA element in the quadruplex-forming region in the c-*MYB* promoter (*50*). Studies have shown that promoter regions harboring G-quadruplex potential also have binding sites for one or more transcription factors (*51−54*). These protein factors may compete for the same or exclusive binding sites. Therefore, the co-occurrence of secondary structure formation and protein−DNA interaction may influence each other to either activate or repress gene expression. Third, the introduction of the third strand (TFO) complementary to the target sequence in the NHE region may result in triplex formation leading to downregulation of the gene (*55, 56*). If C-rich (Py) TFO is used to target the G-rich strand, the Py*Pu•Py triplex formation would occur only at acidic pH and is less likely to form at physiological pH (*57, 58*). But the LNA modified C-rich third strand (Py TFO) can form a stable triplex at physiological pH (*57, 58*) and mediate higher transcriptional suppression. However, our gel experiment indicates that the LNA modified oligonulceotides favor the formation of the duplex DNA and not a triplex band in gel studies, as demonstrated by the absence of a super shifted triplex band. Last, the possibility of strand invasion by the LNA modified complementary strand into the duplex region along with the displacement of the C-rich strand cannot be ruled out. The formation of the LNA/DNA duplex upon invasion can result in the suppression of gene expression.

In the present study, it is difficult to differentiate whether the perturbation of gene expression is due to strand invasion and displacement of the C-rich strand or due to the quadruplex to duplex transition induced by the modified complementary strand. However, in both cases quadruplex formation is prevented, which leads to the inhibition of quadruplex mediated transcription. This ability of duplex invasion is well characterized for PNA (*60*), and studies have shown that homopyrimidine PNAs called openers, invade homopurine stretches in duplex DNA. However, to demonstrate the efficient duplex invasion by LNA would require systematic positioning of LNA modifications. To date, the mechanism by which quadruplexes act as transcriptional repressor or activator motifs is unclear. Our work only suggests that Watson−Crick base pairing can be exploited to affect the molecular recognition of a structure and perturb gene expression.

Human cancers are a consequence of a multistage process involving the activation of oncogenes and/or inactivation of tumor suppressor genes that code for proteins that have multiple roles in complex interaction networks. This has led to the introduction of the concept of oncogene addiction to emphasize the apparent dependency of some cancers on one or few genes for the maintenance of the malignant phenotype (*61, 62*). This phenomenon provides a rationale for targeted molecular therapy to impair the survival and growth of cancerous cells by inactivation of a single oncogene. The most convincing evidence for the concept of oncogene addiction comes from the increasing number of the therapeutic antibodies or drugs that target specific oncogenes in human cancers. In a transgenic mouse model, switching on of the c-*MYC* protoncogene leads to myeloid leukemia. However, switching off this gene leads to growth inhibition, tumor regression, and apoptosis. Genome wide search has shown the potential existence of quadruplexes in the promoter regions of many protoncogenes (*63, 64*). Furthermore, these structures are involved in molecular recognition, function, and disease (*13*). The proposed strategy in our study involving the quadruplex−duplex structural switch mediated gene expression obtained through the oligonucleotide approach can be employed to achieve more effective and selective therapy for specific human cancers (Scheme 1).

CONCLUSIONS

Our in vitro and in vivo experiments concurrently assert that perturbing the c-*MYC* quadruplex and driving it to the duplex state can modulate the downstream gene expression. Our results also demonstrate that the locked nucleic acid (LNA) modified complementary strand possesses superior ability to invade the stable quadruplex and consequently affect quadruplex mediated expression. The presence of the putative quadruplexes in a large number of genomic locations suggests that compounds designed to interfere with quadruplex regulated gene expression may not display high selectivity resulting in nonspecific effects. Our approach offers the possibillity to achieve high selectivity since it employs LNA bases, which display unprecedented hybridization ability (*24, 25*) by utilizing the selectivity and specificity of Watson−Crick base pairing.

ACKNOWLEDGMENT

We thank Dr. Beena Pillai for valuable input and Dr. Shantanu Chowdhury for providing the Del 4 plasmid.

SUPPORTING INFORMATION AVAILABLE

Sequences used in this study, 1D ^{1}H NMR spectrum recorded for the 22-mer c-*MYC* quadruplex, CD spectra of the c-*MYC* quadruplex, UV melting profile of the c-*MYC* quadruplex, fluorescence spectra of dual labeled 22-mer c-*MYC* quadruplex (100 nM) with 5′ fluorescein and 3′ TAMRA, gel electrophoresis for the single labeled 22-mer, sensorgrams obtained by hybridization of the 5′ biotin-c-MYC-Na^+ quadruplex to its unmodified and LNA modified complementary strand, and map of the *c-MYC* promoter showing restriction sites used to generate deletion constructs. This material is available free of charge via the Internet at http://pubs.acs.org.

REFERENCES

1. Schwab, M., Alitalo, K., Klempnauer, K. H., Varmus, H. E., Bishop, J. M., Gilbert, F., Brodeur, G., Goldstein, M., and Trent, J. (1983) Amplified DNA with limited homology to myc cellular oncogene is shared by human neuroblastoma cell lines and a neuroblastoma tumour. *Nature 305*, 245–248.
2. Schwab, M., Varmus, H. E., Bishop, J. M., Grzeschik, K. H., Naylor, S. L., Sakaguchi, A. Y., Brodeur, G., and Trent, J. (1984) Chromosome localization in normal human cells and neuroblastomas of a gene related to c-myc. *Nature 308*, 288–291.
3. Kelly, K., and Siebenlist, U. (1984) The regulation and expression of c-myc in normal and malignant cells. *Annu. Rev. Immunol. 4*, 317–338.
4. Kelly, K., Cochran, B. H., Stiles, C. D., and Leder, P. (1983) Cell-specific regulation of the c-myc gene by lymphocyte mitogens and platelet-derived growth factor. *Cell 35*, 603–610.
5. Vervoorts, J., Lüscher-Firzlaff, J., and Lüscher, B. (2006) The ins and outs of MYC regulation by posttranslational mechanisms. *J. Biol. Chem. 281*, 34725–34729.
6. Marcu, K. B., Bossone, S. A., and Patel, A. J. (1992) myc function and regulation. Annu. Rev. *Biochem. 61*, 809–860.
7. Battey, J., Moulding, C., Taub, R., Murphy, W., Stewart, T., Potter, H., Lenoir, G., and Leder, P. (1983) The human c-myc oncogene: structural consequences of translocation into the IgH locus in Burkitt lymphoma. *Cell 34*, 779–787.
8. Siddiqui-Jain, A., Grand, C. L., Bearss, D. J., and Hurley, L. H. (2002) Direct evidence for a G-quadruplex in a promoter region and its targeting with a small molecule to repress c-MYC transcription. *Proc. Natl. Acad. Sci. U.S.A. 99*, 11593–11598.
9. Phan, A. T., Modi, Y. S., and Patel, D. J. (2004) Propeller-type parallel-stranded G-quadruplexes in the human c-myc promoter. *J. Am. Chem. Soc. 126*, 8710–8716.
10. Blackburn, E. H. (1994) Telomeres: no end in sight. *Cell 77*, 621–623.
11. Sen, D., and Gilbert, W. (1988) Formation of parallel four-stranded complexes by guanine-rich motifs in DNA and its implications for meiosis. *Nature 334*, 364–366.
12. Simonsson, T., Pecinka, P., and Kubista, M. (1998) DNA tetraplex formation in the control region of c-myc. *Nucleic Acids Res. 26*, 1167–1172.
13. Ghosal, G., and Muniyappa, K. (2006) Hoogsteen base-pairing revisited: Resolving a role in normal biological processes and human diseases. *Biochem. Biophys. Res. Commun. 343*, 1–7.
14. Kumari, S., Bugaut, A., Huppert, J. L., and Balasubramanian, S. (2007) An RNA G-quadruplex in the 5′ UTR of the NRAS proto-oncogene modulates translation. *Nat. Chem. Biol 3*, 218–221.
15. Wieland, M., and Hartig, J. S. (2007) RNA quadruplex-based modulation of gene expression. *Chem. Biol. 14*, 757–763.
16. Arora, A., Dutkiewicz, M., Scaria, V., Hariharan, M., Maiti, S., and Kurreck, J. (2008) Inhibition of translation in living eukaryotic cells by an RNA G-quadruplex motif. *RNA 14*, 1290–1296.
17. Sun, H., Yabuki, A., and Maizels, N. (2001) A human nuclease specific for G4 DNA. *Proc. Natl. Acad. Sci. U.S.A. 98*, 12444–12449.

18. Zaug, A. J., Podell, E. R., and Cech, T. R. (2005) Human POT1 disrupts telomeric G-quadruplexes allowing telomerase extension in vitro. *Proc. Natl. Acad. Sci. U.S.A. 102*, 10864–10869.
19. Hurley, L. H., Wheelhouse, R. T., Sun, D., Kerwin, S. M., Salazar, M., Fedoroff, O. Y., Han, F. X., Han, H., Izbicka, E., and Von Hoff, D. D. (2002) G-quadruplexes as targets for drug design. *Pharmacol Ther. 85*, 141–158.
20. Izbicka, E., Wheelhouse, R. T., Raymond, E., Davidson, K. K., Lawrence, R. A., Sun, D., Windle, B. E., Hurley, L. H., and Von Hoff, D. D. (1999) Effects of cationic porphyrins as G-quadruplex interactive agents in human tumor cells. *Cancer Res. 59*, 639–644.
21. Green, J. J., Ladame, S., Ying, L., Klenerman, D., and Balasubramanian, S. (2003) Investigating a quadruplex-ligand interaction by unfolding kinetics. *J. Am. Chem. Soc. 125*, 3763–3767.
22. Marin, V. L., and Armitage, B. A. (2005) RNA guanine quadruplex invasion by complementary and homologous PNA probes. *J. Am. Chem. Soc. 127*, 8032–8033.
23. Roy, S., Tanious, F. A., Wilson, W. D., Ly, D. H., and Armitage, B. A. (2007) High-affinity homologous peptide nucleic acid probes for targeting a quadruplex-forming sequence from a MYC promoter element. *Biochemistry 46*, 10433–10443.
24. Petersen, M., and Wengel, J. (2003) LNA: a versatile tool for therapeutics and genomics. *Trends Biotechnol. 21*, 74–81.
25. Kaur, H., Babu, B. R., and Maiti, S. (2007) Perspectives on chemistry and therapeutic applications of Locked Nucleic Acid (LNA). *Chem. Rev. 107*, 4672–4697.
26. Kaur, H., Arora, A., Wengel, J., and Maiti, S. (2006) Thermodynamic, counterion, and hydration effects for the incorporation of locked nucleic acid nucleotides into DNA duplexes. *Biochemistry 45*, 7347–7355.
27. Kaur, H., Wengel, J., and Maiti, S. (2007) LNA-modified oligonucleotides effectively drive intramolecular-stable hairpin to intermolecular-duplex state. Biochem. *Biophys. Res. Commun. 352*, 118–122.
28. McTigue, P. M., Peterson, R. J., and Kahn, J. D. (2004) Sequence-dependent thermodynamic parameters for locked nucleic acid (LNA)-DNA duplex formation. *Biochemistry 43*, 5388–5405.
29. Torigoe, H., Hari, Y., Sekiguchi, M., Obika, S., and Imanishi, T. (2001) 2′-O 4′-C-methylene bridged nucleic acid modification promotes pyrimidine motif triplex DNA formation at physiological pH: thermodynamic and kinetic studies. *J. Biol. Chem. 276*, 2354–2360.
30. Schmidt, K. S., Borkowski, S., Kurreck, J., Stephens, A. W., Bald, R., Hecht, M., Friebe, M., Dinkelborg, L., and Erdmann, V. A. (2004) Application of locked nucleic acids to improve aptamer in vivo stability and targeting function. *Nucleic Acids Res. 32*, 5757–5765.
31. Cantor, C. R., Warshaw, M. M., and Shapiro, H. (1970) Oligonucleotide interactions. Circular dichroism studies of the conformation of deoxyoligonucleotides. *Biopolymers 9*, 1059–1077.
32. Marky, L. A., Blumenfeld, K. S., Kozlowski, S., and Breslauer, K. J. (1983) Salt-dependent conformational transitions in the self-complementary deoxydodecanucleotide d(CGCAATTCGCG): evidence for hairpin formation. *Biopolymers 9*, 1247–1257.
33. He, T. C., Sparks, A. B., Rago, C., Hermeking, H., Zawel, L., da Costa, L. T., Morin, P. J., Vogelstein, B., and Kinzler, K. W. (1998) Identification of c-MYC as a target of the APC pathway. *Science 281*, 1509–1512.
34. Westerfield, M. (1995) *A Guide for Laboratory Use of Zebrafish (Danio rerio)*, University of Oregon Press, Eugene OR,
35. Hermanson, S., Davidson, A. E., Sivasubbu, S., Balciunas, D., and Ekker, S. C. (2004) Sleeping beauty transposon for efficient gene delivery. *Methods Cell Biol. 77*, 349–362.
36. Hyatt, T. M., and Ekker, S. C. (1999) Vectors and techniques for ectopic gene expression in zebrafish. *Methods Cell Biol. 59*, 117–126.
37. Davidson, A. E., Balciunas, D., Mohn, D., Shaffer, J., Hermanson, S., Sivasubbu, S., Cliff, M. P., Hackett, P. B., and Ekker, S. C. (2003) Efficient gene delivery and gene expression in zebrafish using the Sleeping Beauty transposon. *Dev. Bio. 263*, 191–202.
38. Smith, P. K., Krohn, R. I., Hermanson, G. T., Mallia, A. K., Gartner, F. H., Provenzano, M. D., Fujimoto, E. K., Goeke, N. M., Olson, B. J., and Klenk, D. C. (1985) Measurement of protein using bicinchoninic acid. *Anal. Biochem. 150*, 76–85.
39. Risitano, A., and Fox, K. R. (2003) Stability of intramolecular DNA quadruplexes: comparison with DNA duplexes. *Biochemistry 42*, 6507–6513.
40. Graf, D, Timmons, P. M, Hitchins, M, Episkopou, V, Moore, G, Ito, T, Fujiyama, A, Fisher, A. G, and Merkenschlager, M. (2001) Evolutionary conservation, developmental expression, and genomic mapping of mammalian twisted gastrulation. *Mamm. Genome 12*, 554–560.
41. Langenau, D. M., Traver, D., Ferrando, A. A., Kutok, J. L., Aster, J. C., Kanki, J. P., Lin, S., Prochownik, E., Trede, N. S., Zon, L. I., and Look, A. T. (2003) Myc-induced T cell leukemia in transgenic zebrafish. *Science 299*, 887–890.
42. Feistma, H., and Cuppen, E. (2008) Zebrafish as a cancer model. *Mol. Cancer Res. 6*, 685–694.
43. Kumar, N., and Maiti, S. (2004) Quadruplex to Watson-Crick duplex transition of the thrombin binding aptamer: a fluorescence resonance energy transfer study. *Biochem. Biophys. Res. Commun. 319*, 759–767.
44. Kumar, N., and Maiti, S. (2007) Role of locked nucleic acid modified complementary strand in quadruplex/Watson-Crick duplex equilibrium. *J. Phys. Chem. B 111*, 12328–12337.
45. Halder, K., and Chowdhury, S. (2005) Kinetic resolution of bimolecular hybridization versus intramolecular folding in nucleic acids by surface plasmon resonance: application to G-quadruplex/duplex competition in human c-myc promoter. *Nucleic Acids Res. 33*, 4466–4474.
46. Anantha, N. V., Azam, M., and Sheardy, R. D. (1998) Porphyrin binding to quadrupled T4G4. *Biochemistry 37*, 2709–2714.
47. Pan, D, and Courey, A. J. (1992) The same dorsal binding site mediates both activation and repression in a context-dependent manner. *EMBO J. 11*, 1837–1842.
48. Diamond, M. I., Miner, J. N., Yoshinaga, S. K., and Yamamoto, K. R. (1990) Transcription factor interactions: selectors of positive or negative regulation from a single DNA element. *Science 249*, 1266–1272.
49. Ptashne, M. (2004) *A Genetic Switch: Phage λ Revisited*, 3rd ed., Cold Spring Harbor Laboratory Press, Plainview, NY.
50. Palumbo, S. L., Memmott, R. M., Uribe, D. J., Krotova-Khan, Y., Hurley, L. H., and Ebbinghaus, S. W. (2008) A novel G-quadruplex-forming GGA repeat region in the c-myb promoter is a critical regulator of promoter activity. *Nucleic Acids Res. 36*, 1755–1769.
51. Postel, E. H. (1996) NM23/Nucleoside diphosphate kinase as a transcriptional activator of c-myc. *Curr. Top. Microbiol. Immunol. 213*, 233–252.
52. Postel, E. H., Berberich, S. J., Flint, S. J., and Ferrone, C. A. (1993) Human c-myc transcription factor PuF identified as nm23-H2 nucleoside diphosphate kinase, a candidate suppressor of tumor metastasis. *Science 261*, 478–80.
53. Takimoto, M., Tomonaga, T., Matunis, M., Avigan, M., Krutzsch, H., Dreyfuss, G., and Levens, D. (1993) Specific binding of heterogeneous ribonucleoprotein particle protein K to the human c-myc promoter, in vitro. *J. Biol. Chem. 268*, 18249–18258.
54. Michelotti, E. F., Tomonaga, T., Krutzsch, H., and Levens, D. (1995) Cellular nucleic acid binding protein regulates the CT element of the human c-myc protooncogene. *J. Biol. Chem. 270*, 9494–9499.
55. Cooney, M., Czernuszewicz, G., Postel, E. H., Flint, S. J., and Hogan, M. E. (1988) Site-specific oligonucleotide binding represses transcription of the human c-myc gene in vitro. *Science 241*, 456–459.
56. McGuffie, E. M., and Catapano, C. V. (2002) Design of a novel triple helix-forming oligodeoxyribonucleotide directed to the major promoter of the c-myc gene. *Nucleic Acids Res. 30*, 2701–2709.
57. Kumar, N., Nielsen, K. E., Maiti, S., and Petersen, M. (2006) Triplex formation with alpha-L-LNA (alpha-L-ribo-configured locked nucleic acid). *J. Am. Chem. Soc. 128*, 14–15.
58. Obika, S., Uneda, T., Sugimoto, T., Nanbu, D., Minami, T., Doi, T., and Imanishi, T. (2001) 2′-O 4′-C-Methylene bridged nucleic acid (2′,4′-BNA): synthesis and triplex-forming properties. *Biorg. Med. Chem 9*, 1001–1011.
59. Datta, B., and Armitage, B. A. (2001) Hybridization of PNA to structured DNA targets: quadruplex invasion and the overhang effect. *J. Am. Chem. Soc. 123*, 9612–9619.
60. Bukanov, N. O., Demidov, V. V., Nielsen, P. E., and Frank-Kamenetskii, M. D. (1998) PD-loop: a complex of duplex DNA with an oligonucleotide. *Proc. Natl. Acad. Sci. U.S.A. 95*, 5516–5520.
61. Weinstein, I. B. (2002) Cancer. Addiction to oncogenes-the Achilles heal of cancer. *Science 297*, 63–64.

62. Weinstein, I. B., and Joe, A. K. (2006) Mechanisms of disease: Oncogene addiction-a rationale for molecular targeting in cancer therapy. *Nat. Clin. Pract. Oncol. 3*, 448–457.
63. Huppert, J. L., and Balasubramanian, S. (2005) Prevalence of quadruplexes in the human genome. *Nucleic Acids Res. 33*, 2908–2916.
64. Todd, A. K., Johnston, M., and Neidle, S. (2005) Highly prevalent putative quadruplex sequence motifs in human DNA. *Nucleic Acids Res. 33*, 2901–2907.

BI801064J